Sensitivity-Enhanced Hot-Wire Anemometer by Using Cladding-Etched Fiber Bragg Grating

Yuhan TANG[1,2], Xuke CHEN[3], Jiarui ZHANG[2,4], Dajuan LV[5], Liangming XIONG[5], and Xinyong DONG[2,4,6*]

[1]*School of Physics and Optoelectronic Engineering, Guangdong University of Technology, Guangzhou 510006, China*

[2]*Guangdong Provincial Key Laboratory of Information Photonics Technology, Guangzhou 510006, China*

[3]*Institute of Optoelectronic Technology, China Jiliang University, Hangzhou 310018, China*

[4]*School of Information Engineering, Guangdong University of Technology, Guangzhou 510006, China*

[5]*State Key Laboratory of Optical Fiber and Cable Manufacture Technology, Wuhan 430073, China*

[6]*Southern Marine Science and Engineering Guangdong Laboratory, Zhuhai 519000, China*

[*]Corresponding author: Xinyong DONG E-mail: dongxy@gdut.edu.cn

Abstract: A sensitivity-enhanced hot-wire anemometer based on a cladding-etched optical fiber Bragg grating (FBG) coated with a layer of silver film and optically heated by using a 1480 nm laser diode is demonstrated. The silver film absorbs the laser power to heat the FBG to a certain high temperature and the airflow cools down the FBG hot-wire with the cooling effect and hence the Bragg wavelength of the FBG is determined by the airflow velocity. Experimental measurement results show that the heating efficiency of the FBG hot wire is improved by 3.8 times in magnitude by etching the fiber cladding from 125 μm down to 73.4 μm, and the achieved airflow velocity sensitivities, under a laser power of 200 mW, are –3 180 pm/(m/s), –889 pm/(m/s), –268 pm/(m/s), and –8.7 pm/(m/s) at different airflow velocities of 0.1 m/s, 0.5 m/s, 1.5 m/s, and 17 m/s, respectively. In comparison, the sensitivities are only –2193 pm/(m/s), –567 pm/(m/s), –161 pm/(m/s), and –4.9 pm/(m/s) for the reference anemometer without cladding etching even at a much higher heating laser power of 530 mW. These results prove that the method by using a cladding-etched FBG to improve sensitivity of FBG-based hot-wire anemometers works and the sensitivity is improved significantly.

Keywords: Fiber Bragg grating; hot-wire anemometer; optical fiber sensors

Citation: Yuhan TANG, Xuke CHEN, Jiarui ZHANG, Dajuan LV, Liangming XIONG, and Xinyong DONG, "Sensitivity-Enhanced Hot-Wire Anemometer by Using Cladding-Etched Fiber Bragg Grating," *Photonic Sensors*, 2023, 13(3): 230305.

1. Introduction

Airflow velocity measurement is very important in many fields ranging from athletics to energy and aerospace industries. Hot-wire anemometer, in which a wire element heated electrically or optically to a temperature above the ambient is cooled by the airflow, and the airflow velocity is calculated by the rate of heat loss, and is regarded as a promising resolution with the integrated sensing probe and short response time [1, 2]. Hot-wire anemometers based on optical fibers or fiber-based devices have attracted lots of attentions in recent years due to their many advantages including electrically passive operation, remote sensing capability, high sensitivity, and high adaptability to harsh environments [3–15].

Received: 27 July 2022 / Revised: 10 November 2022

DOI: 10.1007/s13320-023-0676-y
Article type: Regular

Metal film-coated optical fiber Bragg gratings (FBGs) are studied as hot wires which can be heated by using a pump laser and measured through the FBGs' Bragg mode reflection wavelength which has an excellent linear response to temperature [16–23]. The wavelength-encoding property of FBG hot-wire anemometers makes the measurement independent of signal intensity, so high accuracy measurement is guaranteed in principle. However, the sensitivity and measurement range depend greatly on starting temperature of the hot wires, namely, temperature of the hot wire when the airflow velocity is zero. Therefore, how to increase pump efficiency to achieve a high starting temperature with a given pump laser power becomes very important in developing high performance FBG hot-wire anemometers.

In this paper, a simple and effective method is demonstrated to improve the sensitivity of FBG hot-wire anemometers by using a cladding-partially-etched FBG as the hot wire. The FBG is coated with a layer of silver film and optically heated by using a 1480 nm laser diode. The silver film absorbs the laser power to heat the FBG to a certain high temperature and the airflow cools down the FBG hot-wire with the cooling effect determined by the airflow velocity. Experimental results show that the heating efficiency of the FBG hot wire is improved by 3.8 times in magnitude by etching the fiber cladding from 125 μm down to 73.4 μm, and the achieved airflow velocity sensitivities, under a laser power of 200 mW, are –3180 pm/(m/s), –889 pm/(m/s), –268 pm/(m/s), and –8.7 pm/(m/s) at different airflow velocities of 0.1 m/s, 0.5 m/s, 1.5 m/s, and 17 m/s, respectively. In comparison, the sensitivities are only –2193 pm/(m/s), –567 pm/(m/s), –161 pm/(m/s), and –4.9 pm/(m/s) for the reference anemometer without cladding etching even at a much higher laser power of 530 mW.

2. Sensor fabrication and principle

The sensing part of the proposed FBG anemometer is presented schematically in Fig. 1. It is formed by cascading a waist-enlarged optical fiber bitaper with a silver film-coated, cladding-partially-etched FBG. The bitaper, fabricated by using a normal fusion splicer (Fujikura FSM-60s) under the auto-splicing mode with a relatively larger overlap distance of 110 μm, is about 350 μm long with a waist diameter of 141.7 μm. Its insertion loss at the pump wavelength is 13.1 dB, indicating that 95.1% of the input pump laser will be coupled into the fiber cladding due to the deformed geometry of the fiber bitaper. The 4-mm-long FBG, with a center-to-center distance of 7.0 mm to the bitaper, is written in a hydrogen-loaded single-mode fiber (Corning SMF-28) by using a 244 nm ultraviolet laser through a phase mask. Its Bragg wavelength is 1550.03 nm and the reflectivity is 90%. The FBG is then chemically etched by using hydrofluoric acid solution of 20% concentration for a time duration of 120 minutes. The cladding diameter of the FBG is reduced from 125 μm to 73.4 μm. Then, a silver film with thickness of 260 nm is deposited on the surface of the FBG by using the magnetron sputtering method. Finally, a uniform aluminium doped zinc oxide film with a thickness of 80 nm is deposited outside the silver film to prevent it from being oxidized in the air [24].

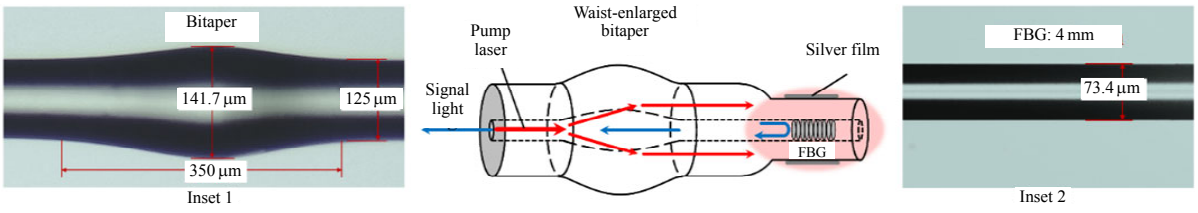

Fig. 1 Schematic diagram of the proposed optical fiber anemometer. Inset 1: micrograph of the waist-enlarged fiber bitaper and Inset 2: micrograph of the etched FBG.

The silver film absorbs the pump laser from the fiber cladding and generates heat. The FBG is heated to a temperature above the air temperature and the cooling effect of the FBG is determined by the airflow velocity. When the airflow velocity is zero, the FBG's temperature, for a given pump laser power, will reach a maximum value where the heat generated by the silver film equals to that escaping from the film to the surrounding air. When such a thermal equilibrium is established, the following relationship can be achieved [25, 26]:

$$P\varphi a_{\mathrm{Ag}} = 2\pi rLh(T_0 - T_e) \tag{1}$$

where P is the power of the pump laser, φ is the coupling coefficient of the waist-enlarged fiber bitaper, a_{Ag} is the absorption coefficient of the silver film to the pump laser, h is the convective heat transfer coefficient, T_0 is the starting temperature, T_e is the air temperature, and $2\pi rL$ is the area of the silver coating film with r and L being the radius and length of the coated FBG, respectively. The left of (1) represents the heat generation due to laser pump and the right represents the heat loss decided by Newton's law of cooling. So, the starting temperature is inversely proportional to the radius of the FBG if other parameters are fixed. If we reduce the radius of the FBG, the starting temperature will be increased consequently.

When air flows through the FBG anemometer, the heat escaping rate will be increased accordingly. As a result, the temperature of the FBG will be decreased and the Bragg wavelength of the FBG will be blue shifted till a new dynamic thermal equilibrium is established. Based on previous studies on FBG-based hot-wire anemometers [27], we can describe the Bragg wavelength of the FBG anemometer as a function of the airflow velocity by [28]

$$\lambda = \lambda_0\left(1 + \frac{kP\varphi a_{\mathrm{Ag}}}{A + Bv^n}\right) \tag{2}$$

where λ_0 is the initial Bragg wavelength of the FBG when there is no laser heating, k is the FBG's temperature coefficient of sensitivity, A and B are empirical calibration constants, n is the exponent, and v is the airflow velocity.

3. Experimental results and discussion

Figure 2 shows the experimental setup of the FBG anemometer. A broadband source (BBS) with the flat output spectrum in the wavelength range of 1 540 nm–1 560 nm and an optical spectrum analyzer (OSA) with a wavelength resolution of 0.03 nm were used to measure the Bragg wavelength shift of the FBG anemometer via an optical circulator. An 1 480 nm laser diode with the maximum output power of 530 mW was used to heat the sensing FBG via a 1480 nm/1550 nm WDM coupler. A wind tunnel with a radius of 2 cm was used to provide a stable air flow with variable velocity up to 17 m/s. For comparison purpose, two more anemometer samples with different cladding diameters of 125 μm and 98.2 μm were tested too.

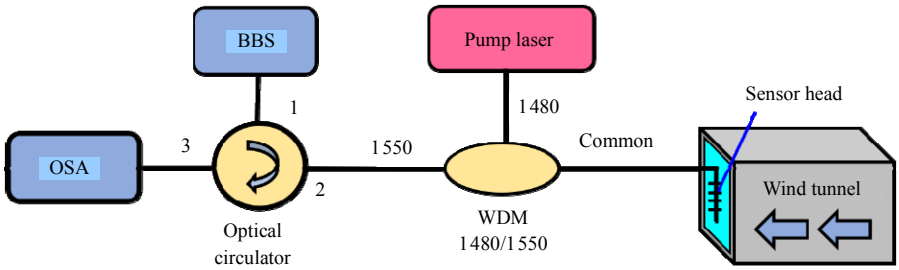

Fig. 2 Experimental setup.

Before airflow velocity testing, we measured reflection spectra of the three FBG anemometer samples with different pump powers. The measured results as shown in Fig. 3(a) indicate obviously that the heating effect of the pump laser to the FBGs is much enhanced by using the cladding-etching

technique. The center wavelength of the FBG anemometer with a diameter of 73.4 μm was red shifted by 2.60 nm, from 1550.03 nm to 1552.63 nm, under pump power of 200 mW. The wavelength shift is much larger than those of the two reference anemometers, which are only 1.80 nm and 1.51 nm for the 98.2 μm and 125 μm diameter ones respectively even at a much higher pump power of 530 mW. Considering the typical temperature sensitivity of 10 pm/℃ for FBGs, temperature increments of 260 ℃, 180 ℃, and 151 ℃ were achieved by laser heating for the three anemometers, respectively.

It also can be seen in Fig. 3(a) that the reflection spectrum for the FBG anemometer with a diameter of 73.4 μm was seriously chirped at 200 mW pump power. The spectrum was much broadened and the reflectivity was reduced seriously by 2.4 dB. The chirp effect should be related to continuous absorption of the pump power which led to a small temperature gradient along the length of the FBG.

Figure 3(b) shows the measured wavelength of the three FBG anemometer samples against pump laser power. Center wavelengths of 3 dB band were adopted rather than peak reflection wavelengths in order to avoid the chirp effect-introduced jump in the peak wavelength. By linear fitting, we achieved the pump or heating efficiencies of 13.0 pm/mW, 3.7 pm/mW, and 2.7 pm/mW for the proposed and the reference anemometers, respectively. It shows clearly that the pump or heating efficiency was improved by 3.8 times and 37% when the FBG diameter was reduced to 73.4 μm and 98.2 μm respectively as against the original 125 μm one. This measurement results confirm the theoretical prediction.

The proposed anemometer was then tested at the pump laser power of 200 mW by using a wind tunnel with changeable airflow velocity between 0 and 17 m/s. Sensor head of the anemometer was inserted into the wind tunnel vertically to the airflow direction. The input fiber end was held tightly and the other end was kept free. Although the sensing fiber was bent slightly by airflow due to air force, the Bragg wavelength of the FBG was not be changed because the mode coupling took place between both core modes. During the measurement, the temperature of the airflow was kept fixed at 25℃.

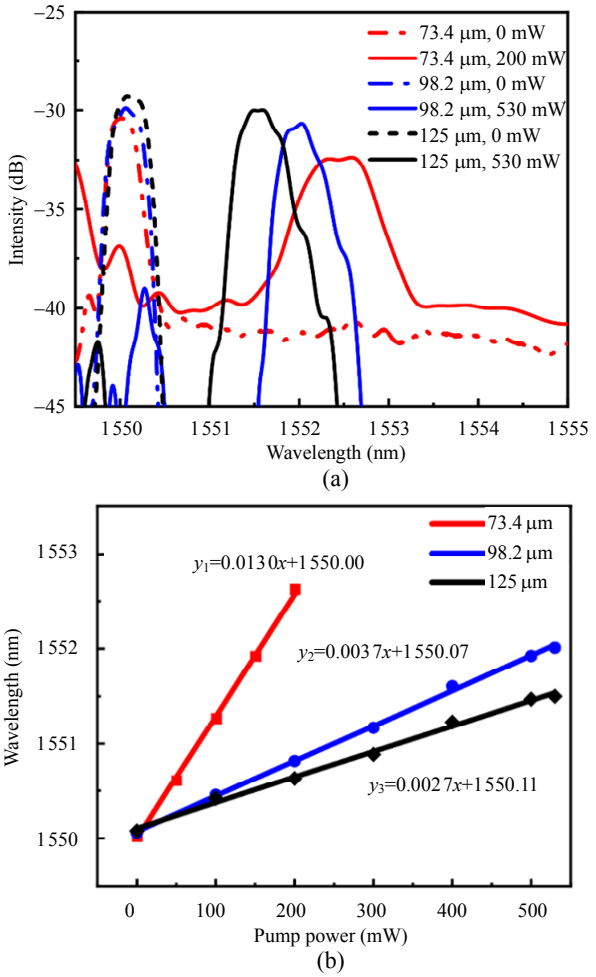

Fig. 3 Comparison of heating efficiency: (a) measured reflection spectra of the three FBG anemometer samples with or without laser heating and (b) measured center wavelength of the three FBG anemometer samples against pump laser power.

When the airflow velocity is increased, the Bragg wavelength of the FBG shifts gradually to the shorter wavelength direction as shown in Fig. 4. Meantime, the reflectivity increases and the bandwidth decreases gradually with the airflow velocity. The spectral profile returns towards the original one when there was no laser heating. This is because the non-uniform heating induced chirp

effect was relieved too with the airflow-induced decrease in average temperature of the FBG.

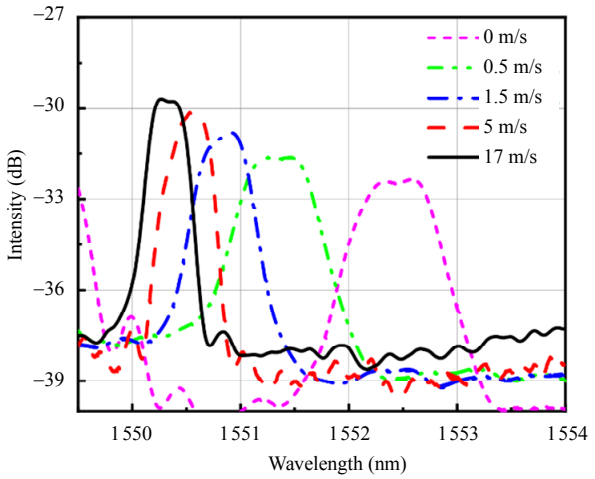

Fig. 4 Reflection spectra of the etched FBG anemometer under various airflow velocities.

When the airflow velocity was changed from 0 to 17 m/s, the Bragg wavelength of the FBG anemometer changes by 2.26 nm, from 1552.63 nm to 1550.37 nm. The measured data of wavelength against the applied airflow velocity for both the proposed and reference anemometers are shown in Fig. 5. After data fitting with the form of (2), we achieved a very close fitting curve for the proposed anemometer, described as

$$\lambda_1 = \frac{1.81}{0.69 + v^{0.68}} + 1550.03 \qquad (3)$$

while for the two reference anemometers, the fitting curves are $\lambda_2 = 1.45/(0.70 + v^{0.74}) + 1550.06$ and $\lambda_3 = 0.98/(0.59 + v^{0.68}) + 1550.08$, respectively.

Based on the above experimentally achieved relationship between the wavelength shift and airflow velocity, we can calculate out the value of the airflow velocity easily from the measured wavelength of the anemometer, by using the following equation:

$$v = \sqrt[0.68]{\frac{1.81}{\lambda_1 - 1550.03} - 0.69}\,. \qquad (4)$$

And the sensitivity of the anemometer, achievable by getting derivative of wavelength with respect to the airflow velocity from (3), can be given by

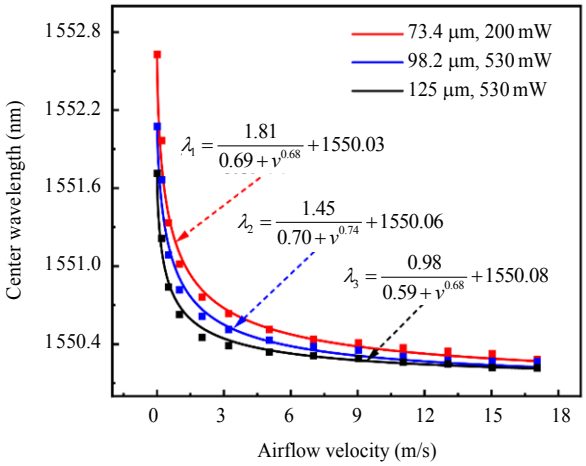

Fig. 5 Measured center wavelength versus applied airflow velocity for the three FBG anemometer samples.

$$\frac{d\lambda_1}{dv} = \frac{-1.23}{v^{0.32}(0.69 + v^{0.68})^2}\,. \qquad (5)$$

The measurement sensitivity depends greatly on the value of the airflow velocity. The smaller the velocity is, the greater the sensitivity becomes. For example, the sensitivity at the airflow velocity of 0.1 nm, 0.5, nm 1.5 nm, and 17 m/s are –3180 pm/(m/s), –889 pm/(m/s), –268 pm/(m/s), and –8.7 pm/(m/s), respectively. The quickly reduced sensitivity with the airflow velocity is related to the Newton's law of cooling, i.e., the surface temperature of an object changes at a rate proportional to the difference between its temperature and the temperature of the surrounding environment. Here, the temperature difference between the FBG and the airflow was reduced quickly from 260 ℃ to 34 ℃ when the airflow velocity was increased from 0 to 17 m/s.

For the purpose of comparison, we calculated the sensitivity of the two reference anemometers based on the derivative of λ_2 and λ_3 versus airflow velocity. For the 98.2 μm one, they are –2510 pm/(m/s), –762 pm/(m/s), –230 pm/(m/s), and –6.6 pm/(m/s) for various airflow velocities of 0.1 m/s, 0.5 m/s, 1.5 m/s, and 17 m/s, respectively. For the 125 μm one, they are –2193 pm/(m/s), –567 pm/(m/s), –161 pm/(m/s), and –4.9 pm/(m/s)

for various airflow velocities of 0.1 m/s, 0.5 m/s, 1.5 m/s, and 17 m/s, respectively. By simple comparison, one can see that the 73.4 μm one possesses all the highest (in magnitude) sensitivity at the four different airflow velocities and the 125 μm one possesses the lowest. Therefore, the sensitivity of the FBG hot-wire anemometer was greatly improved by using the cladding etching technique.

We compared the performances of our proposed FBG hot-wire anemometer with some of the previously reported typical ones and the results are shown in Table 1. It can be seen that our proposed FBG hot-wire anemometer possesses the highest sensitivity.

Table 1 Performance comparison of FBG hot-wire anemometers.

Year	Sensing element	Coupling structure	Coating materials	Measurement range (m/s)	Sensitivity at 0.5 m/s, Abs. [pm/(m/s)]	Reference
2011	FBG	Long period grating	Silver film	0–5	172	[18]
2012	FBG	Core-offset splice	Silver film	0–17.3	45.3	[19]
2013	FBG	No-core fiber	Silver film	0–13.7	193	[20]
2014	FBG	Bitaper	Silver film	0–13.7	299	[27]
2019	FBG	Elliptical core micro-FBG	Graphene	0–1.0	270	[8]
2022	Cladding-etched FBG	Bitaper	Silver film	0–17	889	This work

Abs.: absolution value

Further improvement of performances of the anemometer is expectable if we reduce the fiber diameter of the FBG to a smaller value, but the mechanical strength of the sensing fiber will be reduced. And for quick measurement, commercially available FBG interrogator can be used to replace the bulky and expensive optical spectrum analyzer. By doing so, one can improve the wavelength measurement resolution by one order to pm level and the scanning frequency up to kHz.

4. Conclusions

A simple and effective method to improve performances of FBG-based hot-wire anemometers by using cladding partially etched FBG has been proposed and demonstrated experimentally. The FBG was coated with a layer of silver film and optically heated by using a 1480 nm laser diode to act as the hot-wire. Comparative studies have been carried out and indicated that the heating efficiency of the FBG hot-wire has been increased by 3.8 times by reducing the FBG diameter from 125 μm down to 73.4 μm. As a result, the airflow velocity measurement with improved sensitivities of –3180 pm/(m/s), –889 pm/(m/s), –268 pm/(m/s), and –8.7 pm/(m/s) at different airflow velocities of 0.1 m/s, 0.5 m/s, 1.5 m/s, and 17 m/s have been achieved, respectively. The measurement range, limited by the wind tunnel used in the experiment, was 0–17 m/s. This method is applicable to most of the FBG-based hot-wire anemometers.

Acknowledgment

Sponsor and financial support acknowledgments are placed here. This work was supported by National Key Research and Development Program of China (Grant No. 2020YFB1805804), National Natural Science Foundation of China (Grant No. 11974083), Open Projects Foundation (Grant No. SKLD1905) of State Key Laboratory of Optical Fiber and Cable Manufacture Technology (YOFC), and the Program for Guangdong Introducing Innovative and Entrepreneurial Teams (Grant No. 2019ZT08X340).

References

[1] P. Ligęza, “An investigation of a constant-

bandwidth hot-wire anemometer," *Flow Measurement and Instrumentation*, 2009, 20(3): 116–121.
[2] S. Silvestri and E. Schena, "Micromachined flow sensors in biomedical applications," *Micromachines*, 2012, 3(2): 225–243.
[3] S. Gao, A. P. Zhang, H. Y. Tam, L. H. Cho, and C. Lu, "All-optical fiber anemometer based on laser heated fiber Bragg gratings," *Optics Express*, 2011, 19(11): 10124–10130.
[4] R. Chen, A. Yan, Q. Wang, and K. P. Chen, "Fiber-optic flow sensors for high-temperature environment operation up to 80℃," *Optics Letters*, 2014, 39(13): 3966–3969.
[5] G. Liu, W. Hou, W. Qiao, and M. Han, "Fast-response fiber-optic anemometer with temperature self-compensation," *Optics Express*, 2015, 23(10): 13562–13570.
[6] R. Gao, D. Lu, J. Cheng, and Z. Qi, "Real-time fiber-optic anemometer based on a laser-heated few-layer graphene in an aligned graded-index fiber," *Optics Letters*, 2017, 42(14): 2703–2706.
[7] F. Wang, Y. Duan, M. Lu, Y. Zhang, Z. Jing, C. Sun, *et al.*, "Linear-response and simple hot-wire fiber-optic anemometer using high-order cladding mode," *Optics Express*, 2020, 28(18): 27028–27036.
[8] R. Gao and D. F. Lu, "Temperature compensated fiber optic anemometer based on graphene-coated elliptical core micro-fiber Bragg grating," *Optics Express*, 2019, 27(23): 34012–34022.
[9] J. Zhang, X. Dong, P. Xu, D. Lv, J. Yang, and Y. Qin, "Optical fiber thermal anemometer with light source-heated Fabry-Perot interferometer," *Journal of Lightwave Technology*, 2022, 40(9): 3010–3015.
[10] F. Wang, Y. Duan, M. Lu, Y. Zhang, Z. Jing, C. Sun, *et al.*, "Fiber-optic hot-wire anemometer with directional response based on symmetry-breaking induced heat transfer mechanism," *Journal of Lightwave Technology*, 2021, 39(12): 3919–3925.
[11] Z. Liu, F. Wang, Y. Zhang, Z. Jing, and W. Peng, "Low-power-consumption fiber-optic anemometer based on long-period grating with SWCNT coating," *IEEE Sensors Journal*, 2019, 19(7): 2592–2597.
[12] Y. Zhang, F. Wang, Z. Liu, Z. Duan, W. Cui, J. Han, *et al.*, "Fiber-optic anemometer based on single-walled carbon nanotube coated tilted fiber Bragg grating," *Optics Express*, 2017, 25(20): 24521–24530.
[13] C. L. Lee, K. W. Liu, S. H. Luo, M. S. Wu, and C. T. Ma, "A hot-polymer fiber Fabry-Perot interferometer anemometer for sensing airflow," *Sensors*, 2017, 17(9): 2015.
[14] Y. Zhao, H. Hu, D. Bi, and Y. Yang, "Research on the optical fiber gas flowmeters based on intermodal interference," *Optics and Lasers in Engineering*, 2016, 82: 122–126.
[15] M. Wylie, A. Brown, and B. Colpitts, "Distributed hot-wire anemometry based on Brillouin optical time-domain analysis," *Optics Express*, 2012, 20(14): 15669–15678.
[16] L. J. Cashdollar and K. P. Chen, "Fiber Bragg grating flow sensors powered by in-fiber light," *IEEE Sensors Journal*, 2005, 5(6): 1327–1331.
[17] C. M. Jewart, B. McMillen, S. K. Cho, and K. P. Chen, "X-probe flow sensor using self-powered active fiber Bragg gratings," *Sensors and Actuators A: Physical*, 2006, 127(1): 63–68.
[18] P. Caldas, P. Jorge, G. Rego, O. Frazão, J. Santos, L. Ferreira, *et al.*, "Fiber optic hot-wire flowmeter based on a metallic coated hybrid long period grating/fiber Bragg grating structure," *Applied Optics*, 2011, 50(17): 2738–2743.
[19] X. Dong, Y. Zhou, W. Zhou, J. Cheng, and Z. Su, "Compact anemometer using silver-coated fiber Bragg grating," *IEEE Photonics Journal*, 2012, 4(5): 1381–1386.
[20] X. Wang, X. Dong, Y. Zhou, K. Ni, J. Cheng, and Z. Chen, "Hot-wire anemometer based on silver-coated fiber Bragg grating assisted by no-core fiber," *IEEE Photonics Technology Letters*, 2013, 25(24): 2458–2461.
[21] J. Wang, Z. Liu, S. Gao, A. Zhang, Y. Shen, and H. Tam, "Fiber-optic anemometer based on Bragg grating Inscribed in metal-filled microstructured optical fiber," *Journal of Lightwave Technology*, 2016, 34(21): 4884–4889.
[22] G. Berruti, P. Vaiano, A. Boniello, S. Principe, G. Quero, G. Persiano, *et al.*, "Highly efficient fiber optic thermal heating device based on turn-around-point long period gratings," *Journal of Lightwave Technology*, 2022, 40(3): 797–804.
[23] A. Garcia-Ruiz, A. Dominguez-Lopez, J. Pastor-Graells, H. Martins, S. Martin-Lopez, and M. Gonzalez-Herraez, "Long-range distributed optical fiber hot-wire anemometer based on chirped-pulse ΦOTDR," *Optics Express*, 2018, 26(1): 463–476.
[24] J. Y. Kim, M. J. Park, and J. H. Lee, "Effect of Al_2O_3/ZnO nanolaminate by atomic layer deposition (ALD) on p-Si photocathode for photoelectrochemical hydrogen evolution," *Science of Advanced Materials*, 2015, 7(11): 2492–2495.
[25] Z. Li, J. Wang, T. Liu, L. Zhao, T. Sun and K. T. V. Grattan, "High-sensitivity "hot-wire"-based gas velocity sensor for safe monitoring in mining applications," *IEEE Sensors Journal*, 2018, 18(24): 10192–10198.
[26] H. Bruun, *Hot-wire anemometry: principles and signal analysis*. New York: Oxford University Press, 1995.
[27] X. Wang, X. Dong, Y. Zhou, Y. Li, J. Cheng, and Z. Chen, "Optical fiber anemometer using silver-coated fiber Bragg grating and bitaper," *Sensors and Actuators A: Physical*, 2014, 214: 230–233.
[28] B. Han, Y. N Zhang, X. Wang, D. Yang, Y. Liu, J. C. Sun, *et al.*, "High-sensitive fiber anemometer based on surface plasmon resonance effect in photonic crystal fiber," *IEEE Sensors Journal*, 2019, 19(9): 3391–3398.